EurJOC European Journal of Organic Chemistry

FULL PAPER

DOI: 10.1002/ejoc.201200801

Configurationally Stable Tris(tetrathioaryl)methyl Molecular Propellers

Benoît Driesschaert,[a,b] Raphaël Robiette,[a] Cécile S. Le Duff,[a] Laurent Collard,[a] Koen Robeyns,[a] Bernard Gallez,[b] and Jacqueline Marchand-Brynaert*[a]

Keywords: Isomerization / Molecular propeller / EXSY / CSP-HPLC / Density functional calculations / Conformation analysis

Tris(tetrathioaryl)methanols and tris(tetrathioaryl)methanes are direct precursors and metabolites, respectively, of tris(tetrathioaryl)methyl radicals, which are very attractive paramagnetic spin probes for many magnetic resonance applications. Due to steric hindrance, these propeller-shaped molecules display slow interconversion between their two enantiomeric conformations (right-handed and left-handed propeller conformations). Syntheses and HPLC resolutions carried out on a chiral stationary phase have been achieved. The influence of the hybridization of the central carbon atom as well as the *para* substitutient on the conformational stability were experimentally and theoretically studied. Depending on their particular structure, the free activation energy for the isomerization process determined by kinetics of racemization varies from 24.4 to 26.4 kcal mol^{-1} and corresponds to racemization half-lives of 12 and 343 h, respectively. Computational and NOESY/exchange spectroscopy (EXSY) studies are consistent with a two-ring flip mechanism for the isomerization process of tris(tetrathioaryl)methanols, radicals and tris(tetrathioaryl)methanes.

Introduction

Stable tris(tetrathioaryl)methyl radicals are members of a family of trityl radicals that have found many magnetic resonance (MR) applications during the last decade. Their structures were inspired by Gomberg's trityl radical, in which each phenyl group has been *ortho*- and *meta*-substituted by sulfur groups and *para*-substituted by a carboxylic acid group (Figure 1). These modifications were made in order to avoid hydrogen hyperfine splittings, to enhance stability by electronic and steric effects and finally to make these molecules water-soluble. These radicals, initially developed by Nycomed Innovation to be used as hyperpolarizing agents for Overhauser magnetic resonance imaging (OMRI),[1] possess exceptional properties. They exhibit a single sharp electron paramagnetic resonance (EPR) line of less than 10 μT in deoxygenated water, which is typically one order of magnitude less than that of nitroxide radicals, which represent the second class of soluble spin probes used for biomedical EPR. As a result, the sensitivity of detection is very high, because the signal intensity is inversely proportional to the square of the linewidth. In addition, depending on their particular structure, the half-lives in human blood of tris(tetrathioaryl)methyl radicals at 37 °C vary from a few hours to more than 24 h. Finally, they display a low concentration-dependent broadening of their EPR line.[2,3] Due to these unprecedented properties, original Nycomed's and newly synthesized tris(tetrathioaryl)-methyl radicals have been used as spin probes for electron paramagnetic resonance imaging (EPRI),[4] for the measurement of oxygen,[5] pH[6,7] thiol,[8] superoxide anion,[9] redox status[10] and for dynamic nuclear polarization (DNP).[11]

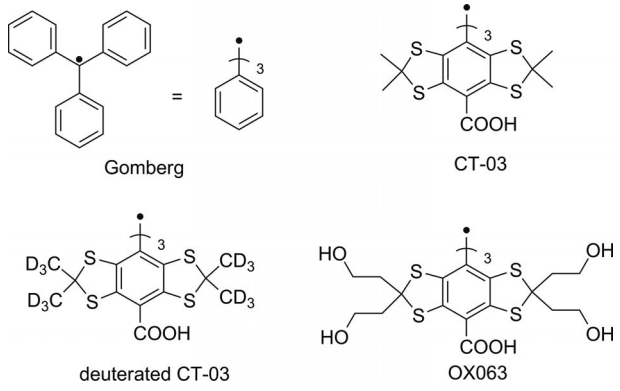

Figure 1. Gromberg's trityl and representative Nycomed's tris(tetrathioaryl)methyl radicals of biomedical uses.

[a] Institute of Condensed Matter and Nanosciences (IMCN), Molecules, Solids and Reactivity (MOST), Université catholique de Louvain,
Place Louis Pasteur 1, L4.01.02, 1348 Louvain-la-Neuve, Belgium
Fax: +32-10-474168
E-mail: jacqueline.marchand@uclouvain.be
Homepage: http://www.uclouvain.be/en-267015.html
[b] Louvain Drug Research Institute (LDRI), Biomedical Magnetic Resonance Section (REMA), Université catholique de Louvain,
avenue Mounier 73, B1.73.08, 1200 Bruxelles, Belgium

Supporting information for this article is available on the WWW under http://dx.doi.org/10.1002/ejoc.201200801.

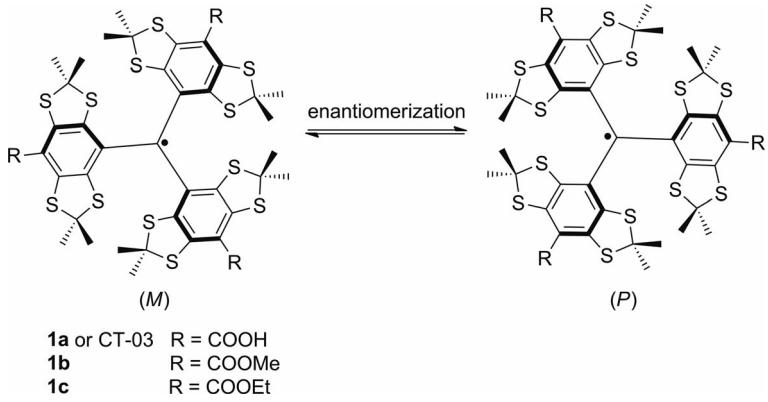

Figure 2. Two enantiomeric conformations of tris(tetrathioaryl)methyl radicals.

A planar conformation would allow the maximum resonance. However, due to steric hindrance, trityl radicals adopt a propeller-like conformation in which all rings have the same direction of twist. This conformation was suggested by Lewis et al. in 1944 based on UV spectra[12] and confirmed later by other techniques (X-ray diffraction,[13] EPR spectrsoscopy,[14] etc.). Tris(tetrathioaryl)methyl radicals are sterically crowded with two five-membered rings on each phenyl ring. This results in a high twist angle, lowering the conjugation of the central carbon atom that consequently bears most of the spin density of the unpaired electron.[3] The X-ray structure of **1b**[15], which is the methyl ester derivative of CT-03 (Figure 2), shows that the rings are twisted by 45.6° relative to the plane of the central carbon atom and its three bonds. This arrangement allows two conformations to occur, namely the right-handed (*P*) and left-handed (*M*) propeller conformations (Figure 2).

These two conformations have an enantiomeric relationship. The study of static and dynamic stereochemistry of three-bladed propellers was launched by Mislow and coworkers more than 30 years ago.[16] In most cases, three-bladed propellers have a low isomerization barrier, which prevents the separation of stereoisomers. However, a few examples of configurationally stable three-bladed propellers bearing bulky aromatic moieties have been reported in the literature, and the stereoisomers could be isolated in optically pure form in some cases.[17,18] Recently, we reported that tris(tetrathioaryl)methyl radicals and their direct diamagnetic precursor tris(tetrathioaryl)methanols[19] (Figure 3) are chiral molecules at room temperature. The propeller-shape conformation associated with a slow interconversion is responsible for this chirality. Semipreparative HPLC carried out on a chiral stationary phase (CSP) allowed the isolation of the two enantiomers of radical **1c** and alcohol **2c**. The half-life of racemization determined for radical **1c** in EtOAc at room temperature is ca. 15 d. This result could have important consequences, because enantiomers can exhibit different biological properties; furthermore, diastereoisomers are formed if a chiral group is connected to the trityl core[10,20] with possibly different physical, biological and chemical properties.

Very recently Tormyshev et al. used exchange spectroscopy (NOESY/EXSY) to study the enantiomerization of tris(tetrathioaryl)methanols **2d** and **2e** (Figure 3); the half-life of racemization at room temperature for **2d** in [D_6]-dimethyl sulfoxide (DMSO) is 8.4 h. For **2e**, a high influ-

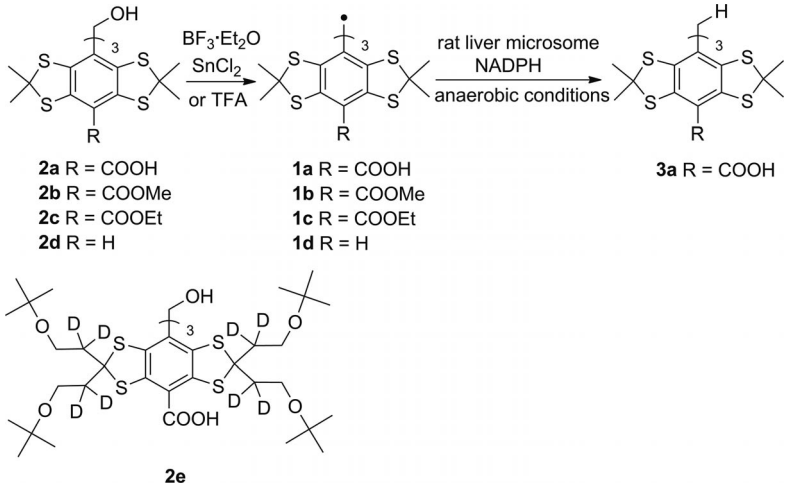

Figure 3. Structures of a few tris(tetrathioaryl)methanols, radicals and a tris(tetrathioaryl)methane.

ence of the steric hindrance of the side-ring was observed.[21] This compound shows a higher conformational stability, and the racemization half-life under the same conditions is 1.36 years. However, no information has been reported concerning the influence of *para* substitution or the enantiomerization of tris(tetrathioaryl)methanes, which are metabolites of radicals produced under reducing conditions.[22]

Herein, we report studies on the dynamic stereochemistry of propeller-shaped tris(tetrathioaryl)methyl radicals, tris(tetrathioaryl)methanols and -methanes. DFT and experimental approaches are used in order to gain insight into the nature of the mechanism of stereoisomerization. The influence of *para* substitution and the hybridization of the central carbon atom are also discussed.

Results and Discussion

Synthesis

The synthesis of **1** and **2** has already been reported.[15,21,23,24] Compound **3c** was synthesized by the reduction of the corresponding alcohol **2c** using trifluoroacetic acid (TFA) and metallic zinc (Figure 4) and was isolated in 50% yield after purification by HPLC. It is known that tris(tetrathioaryl)methanols are quantitatively converted into radicals by TFA,[24] the radical being subsequently reduced by Zn; the resulting anion is protonated by TFA leading to the tris(tetrathioaryl)methane **3c**.

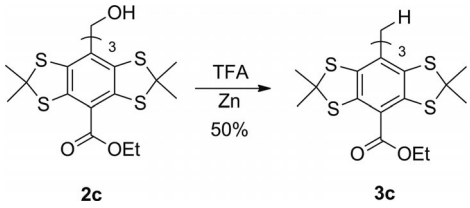

Figure 4. Synthesis of **3c**.

Propeller-Shape Conformation

The ^{1}H NMR spectra of diamagnetic tris(tetrathioaryl)-methanols **2** and -methanes **3** show, except for accidental isochrony, four resonances associated with the methyl groups of the thioacetonide moieties. The nonequivalence of the four methyl groups is consistent with a propeller-shape conformation with C_3 symmetry. In this conformation, the three aryl groups are equivalent, but the four methyl groups of each aryl group are magnetically different as they are localized in different spatial environments. The same observation can be made on the ^{13}C NMR spectra where four resonances are observed for the methyl groups, six for the phenyl rings and two for the quaternary carbon atom of the thioacetonide.

Crystallization from tetrahydrofuran (THF) afforded crystals of alcohol **2d** suitable for X-ray diffraction. The structure reveals a propeller-like conformation and two molecules of cocrystallized THF (Figure 5). As expected the right- and the left-handed propellers are present in the crystal. The three aromatic moieties are twisted in the same direction; however, the structure lacks an exact threefold symmetry. The three dihedral angles θ_1–θ_3, defined as the angle between the two nearest C_{ipso}–C_{ortho} bonds of two adjacent rings, are different (Table 1). A difference in the bond length between the central carbon atom and the three aromatic rings is also observed. In addition, the two five-membered rings connected to the phenyl ring are twisted in the opposite direction for two of the three phenyl rings, whereas they are twisted in the same direction for the last one.

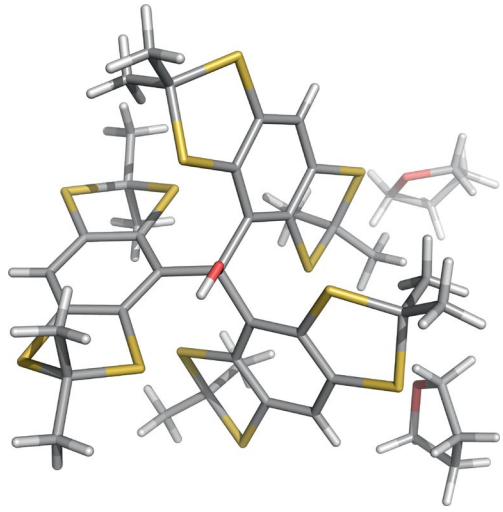

Figure 5. PYMOL view of the structure of **2d** in the crystal.

Table 1. Crystallographic data.

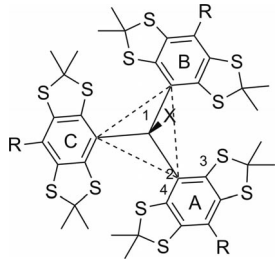

Compd.	R X	θ_1 (C_{A3}–C_{A2}–C_{B2}–C_{B4}) θ_2 (C_{B3}–C_{B2}–C_{C2}–C_{C4}) θ_3 (C_{C3}–C_{C2}–C_{A2}–C_{A4})	d(C_1–C_{2A}) d(C_1–C_{2B}) d(C_1–C_{2C})	Ref.
2d	R = H X = OH	–70.7(4)° –69.9(4)° –75.3(4)°	1.550(6) Å 1.546(6) Å 1.561(5) Å	
1b	R = COOMe X = single electron	–74.0(3)° –74.0(3)° –74.0(3)°	1.449(3) Å 1.449(3) Å 1.449(3) Å	[15]
1e	R = NO_2 X = single electron	–72.3(4)° –86.6(4)° –71.9(4)°	1.450(7) Å 1.468(6) Å 1.461(6) Å	[25]

The X-ray data are available in the literature for the paramagnetic derivatives **1b**[15] and **1e**.[25] Although the methyl ester derivative **1b** exhibits a strict C_3 rotation axis, the nitro derivatives **1e** partly diverge from C_3 symmetry as the

phenyl rings are twisted with three different angles (Table 1). The three bonds connecting the phenyl rings to the central carbon atom also have a slightly different length. However, all the dihedral angles θ_1–θ_3 have the same sign, which reveals a propeller conformation.

Resolution by CSP-HPLC

The resolution of two peaks for tris(tetrathioaryl)methyl radical **1c** and tris(tetrathioaryl)methanol **2c** on HPLC carried out with a cellulose carbamate CSP (CHIRALPAK IB) was the first experimental proof of the chirality of the tris(tetrathioaryl)methyl compounds (Figure 6).[26] The resolution for tris(tetrathioaryl)methane **3c** is also possible at room temperature (Figure 6), indicating that there is no rapid isomerization on the HPLC timescale for the reduced derivative either. The resolutions of ethyl ester derivatives (R = COOEt) **1c**, **2c** and **3c** were achieved by using a cellulose carbamate chiral stationary phase (CHIRALPAK IB), but this column failed to separate the enantiomers of the unsubstituted derivatives **2d** (R = H). The resolution of **2d** was in fact achieved by using an amylose carbamate CSP (CHIRALPAK IA) (Figure 6).

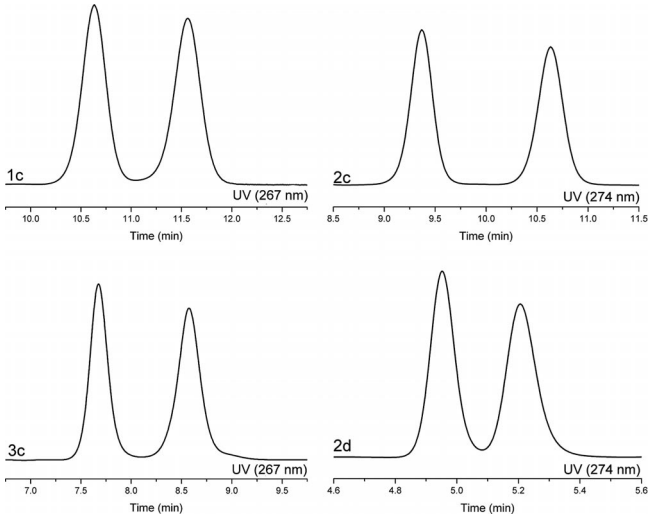

Figure 6. CSP-HPLC chromatograms with UV detection. Resolution was carried out with a CHIRALPAK IB column for **1c**, **2c**, **3c** and on a CHIRALPAK IA column for **2d**.

In order to further evaluate the influence of the hybridization of the central carbon atom and substitutions on the conformational stability, semipreparative resolution of tris(tetrathioaryl)methanols **2c** and **2d** and tris(tetrathioaryl)methane **3c** was undertaken. A few milligrams of each enantiomer of alcohol **2c** was obtained with an enantiomeric ratio (*e.r.*) of 100:0 using semipreparative HPLC (CHIRALPAK IB 10 × 250 mm, 5 μm) according to a procedure previously reported.[26] The semipreparative HPLC resolution of **3c** affords the two optically enriched enantiomers in milligram scale. The first eluted enantiomer was isolated with an *e.r.* of 88.4:11.6, whereas the second eluted enantiomer was isolated with an *e.r.* of 94.0:6.0 using a semipreparative column (CHIRALPAK IB 10 × 250 mm, 5 μm). The amount of each enantiomer that can be isolated is limited by the low solubility of **2c** and **3c** in the eluent. The resolution of unsubstituted alcohol **2d** was carried out on an analytical column (CHIRALPAK IA 4.6 × 250 mm, 5 μm). Half a milligram of each of the two enantiomers was isolated with an *e.r.* of 85.6:14.4 for both enantiomers.

Determination of Configurational Stability

A free activation energy of $\Delta G^{\ddagger}_{(25\,^{\circ}C)} = 26.4\ kcal\,mol^{-1}$ for the enantiomerization process of radical **1c** was determined by monitoring the kinetics of racemization after isolation of the enantiomers.[26] This value is sufficiently high to enable the two enantiomers to be stored independently for months in the freezer. The kinetics of resolution have been extended to methanols **2c** and **2d** and to methane **3c** in order to determine the influence of the nature of the central carbon atom and the influence of aromatic substitution (Table 2). The racemization was monitored by HPLC at 25 °C in EtOAc for each compound (Figure 7). The racemization rates were determined by fitting the experimental

Table 2. Kinetic parameters and enantiomerization free activation energy for **1c**, **2c**, **2d** and **3c** at 25 °C.

Compd.	$k_{rac.}$ [h^{-1}]	$t_{(1/2)rac.}$ [h]	$k_{enant.}$ [h^{-1}]	$\Delta G^{\ddagger}_{enant.}$ [kcal mol^{-1}]	Method
1c[a] (in EtOAc)	0.0020	343.3	0.0010	26.4	HPLC
2c (in EtOAc)	0.0410	16.9	0.0205	24.6	HPLC
2d[b] (in [D_6] DMSO)	0.0823	8.4	0.0411	24.2	NOESY/EXSY
2d (in EtOAc)	0.0572	12.1	0.0286	24.4	HPLC
3c (in EtOAc)	0.0513	13.5	0.0257	24.5	HPLC

[a] Ref.[26] [b] Ref.[21]

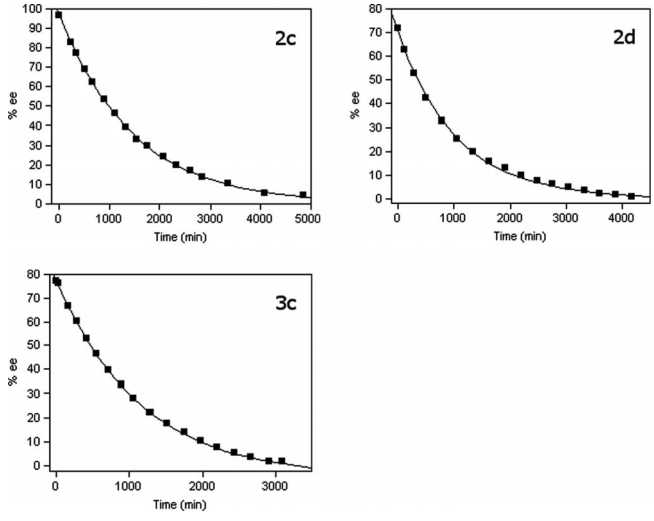

Figure 7. CSP-HPLC kinetics of racemization for **2c**, **2d** and **3c**.

decay of enantiomeric excess (% *ee*) according to Equation (1).

$$\%\ ee = \%\ ee_0 \cdot e^{-k_{rac}t} \quad (1)$$

The racemization and enantiomerization processes are closely linked. The racemization corresponds to a macroscopic and nonreversible process leading to an enantiomeric excess of 0%, which is the thermodynamic equilibrium. The enantiomerization is related to a microscopic and reversible process, which is completed when all of the molecules have been converted into the other enantiomer. The relationship between the rate constants is $k_{rac.} = 2\ k_{enant.}$ The experimental rates of racemization are very close for all diamagnetic compounds **2c**, **2d**, and **3c**, which indicates that there is no strong influence of the *para* substituent (H or COOEt) or of the nature of the group connected to the central carbon atom (H or OH) on the isomerization process. The half-lives of racemization in EtOAc vary from 12.1 h for **2d** to 16.9 h for **2c**; the isomerization rate of **2d** in EtOAc found by CSP-HPLC is in good agreement with the rate found by Tormyshev et al. in DMSO using exchange spectroscopy.[21] However, the rate of isomerization is one order of magnitude lower for the paramagnetic derivative **1c**.

Determination of the Isomerization Mechanism by Exchange Spectroscopy

The isomerization for three-bladed propellers can be described by the so-called Kurland's flip mechanism.[16] There are four pathways leading to helicity reversal, namely, the zero-, one-, two- and three-ring flips. These mechanisms involve a conrotatory rotation of zero, one, two or three aromatic rings across a plane perpendicular to the one formed by the three C_{ipso} atoms (the reference plane) while the other rings rotate in the opposite direction, through the reference plane (Figure 8). The two-ring flip is considered as

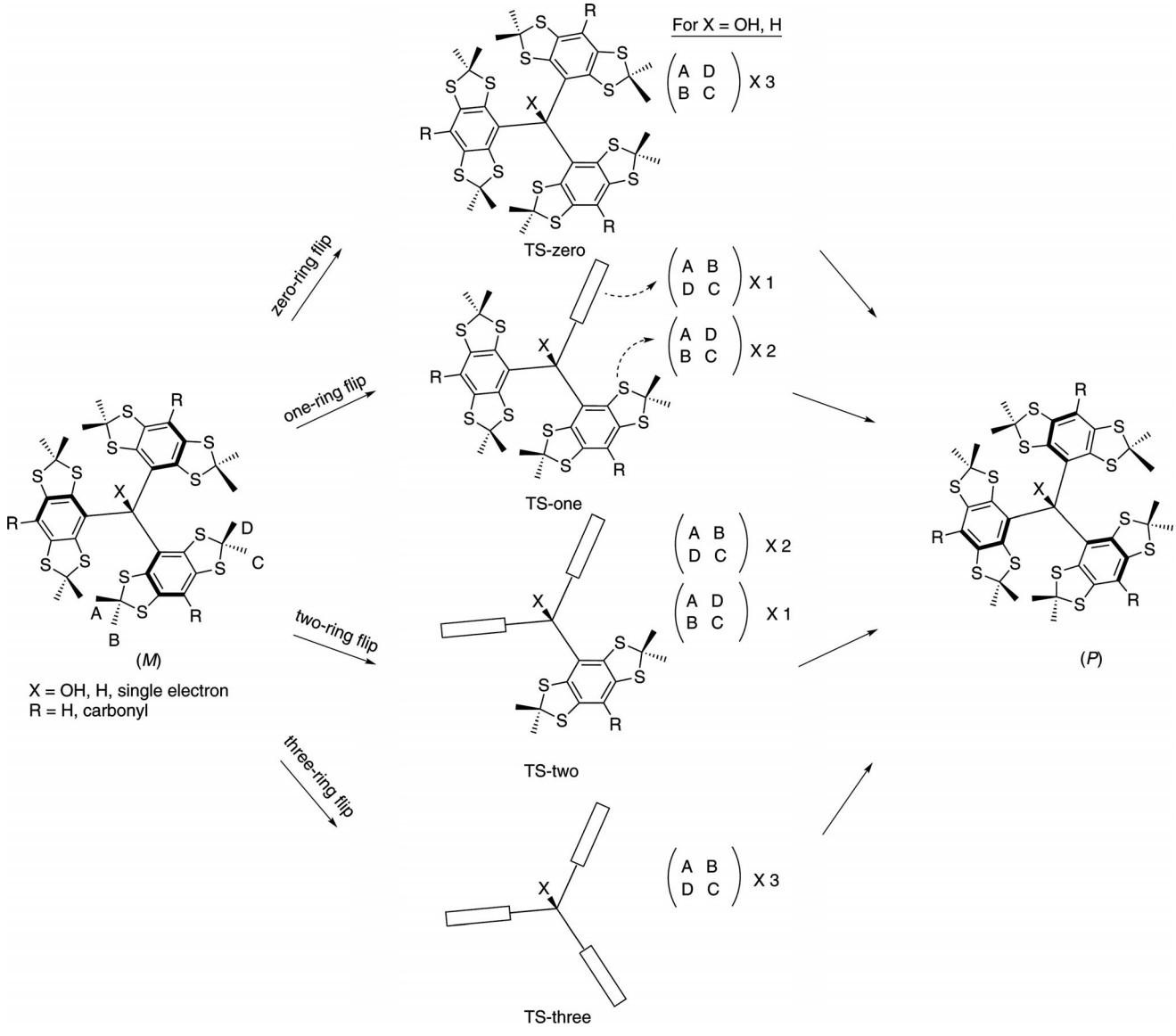

Figure 8. *n*-Ring-flip mechanisms and exchanged positions.

the lower-energy mechanism for the helicity reversal; however, exceptions exist.[27]

In the case of a tetrahedral configuration of the central carbon atom for diamagnetic **2** (X = OH) and **3** (X = H), the four methyl groups (A, B, C, D, Figure 8) are localized in different spatial environments, resulting in four distinct peaks in the ^{1}H and ^{13}C NMR spectra. Degeneracy arises for the radical derivatives **1**, the planar geometry of the central carbon atom makes the methyl groups A equivalent to C and the methyl groups B equivalent to D. Analysis of isomerization mechanisms for tris(tetrathioaryl)methyl derivatives **2** and **3** shows an exchange of the position of methyl groups A and B and an exchange of position of methyl groups D and C when the rings rotate through the plane perpendicular to the reference plane, whereas the rotation in the opposite direction involves an exchange of the position of methyl groups A and D and methyl groups B and C. Tormyshev et al. used exchange spectroscopy to determine the ratio of flipping rings passing through the plane perpendicular to the reference plane to rings flipping through the reference plane.[21] A ratio of 2:1 was determined for tris(tetrathioaryl)methanol **2d**, which corresponds to a two-ring flip mechanism.

A similar strategy to determine the mechanism of isomerization of tris(tetrathioaryl)methane **3c** was used. The ^{1}H NMR spectrum of **3c** at 500 MHz shows four resonances for the methyl groups in deuterated chloroform but only three in [D$_6$]DMSO because of accidental isochrony of two methyl groups. However, by increasing the temperature, a small change in peak frequency is observed leading to complete resolution of the methyl groups. Correlations in the 2D ^{1}H-^{13}C HMBC spectrum reveal that methyl groups 1 and 2 (Figure 9) are attached to the same carbon atom; in the same fashion methyl groups 3 and 4 are attached to the same carbon atom.

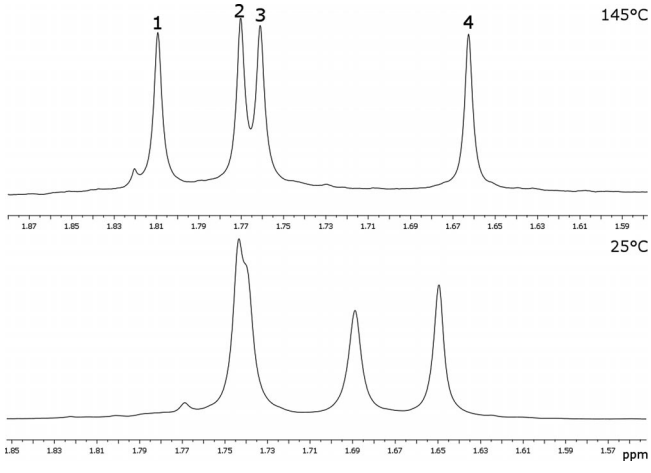

Figure 9. Expansion of the methyl group region of **3c** in [D$_6$]DMSO at 25 and 145 °C (500 MHz).

A high-resolution 2D ^{1}H-^{1}H NOESY/EXSY spectrum was recorded at 145 °C in [D$_6$]DMSO with a spectrometer operating at 500 MHz for ^{1}H, with mixing time of 600 ms. The acquisition region was centred on the methyl groups with a spectral width of 0.5 ppm in both *F*1 and *F*2 dimensions. In such spectra, cross-peaks that have the same sign as the diagonal are chemical exchange peaks (EXSY), whereas cross-peaks that have a sign opposite to the diagonal are nuclear Overhauser effect (nOe) peaks (NOESY). At 145 °C, eight correlations with the same sign as the diagonal are observed corresponding to chemical exchange (Figure 10). As the 2D NOESY/EXSY spectrum is symmetrical across the diagonal, the same information is found twice on such a spectrum, so it is only essential to describe four of the eight correlations. First of all, an EXSY cross-peak is observed between geminal methyl groups 4 and 3 with an intensity of two, whereas an EXSY cross-peak is observed between methyl groups 4 and 1 with an intensity of one. Furthermore, two EXSY cross-peaks are obtained for methyl group 3, one with methyl group 4 (intensity two) and one with methyl group 2 (intensity one). For each methyl group, there is exchange between its geminal position with an intensity of two, which corresponds to a rotation across the plane perpendicular to the reference plane and exchange with a position on the opposite side of the aryl moiety with an intensity of one, which corresponds to the rotation through the reference plane. The only mechanism that fits these observations is the two-ring flip mechanism (Figure 8).

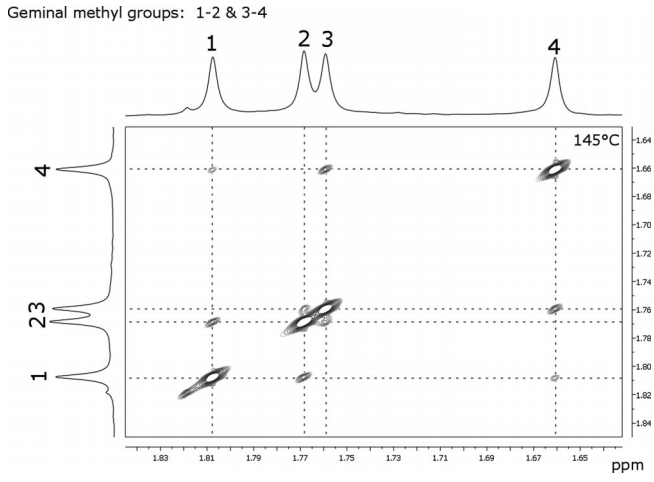

Figure 10. 2D ^{1}H-^{1}H NOESY/EXSY spectrum of **3c** at 145 °C (500 MHz).

Computational Chemistry

We first investigated the mechanism of isomerization by exploring the four potential pathways for interconversion for radical (**1d**) and alcohol (**2d**) derivatives using DFT methods. Transition-state (TS) structures could be found for the two- and three-ring flip mechanisms. For the other mechanisms (zero- and one-ring flip), our calculations revealed that bringing two of the aromatic rings in the same plane would lead to such a spatial proximity between the thio substituents of these aryl groups (< 0.5 Å between two S atoms) that these structures are simply not realistic. The calculated energies of the transition states confirm that the

lower-lying pathway for helicity reversal is, in both cases, the one involving a two-ring flip mechanism (Table 3). This can be accounted for by the difference in steric strain between the two transition-state structures. Indeed, the three-ring flip TS involves a close proximity of *ortho*-thio substituents of the three aromatic rings, which highly destabilizes this structure. In the case of radical **1d**, there is also a difference in spin delocalization between the two- and three-ring flip TS structures; the two-ring flip TS allows delocalization of spin density into one aromatic ring, whereas in the three-ring flip TS the three aromatic rings are perpendicular to the reference plane preventing any conjugation (Figure 11). Stabilization by delocalization into one aromatic ring can be estimated by computing the energy barrier of rotation around the CH_2–Ar single bond of the model paramagnetic 2,2,6,6-tetramethylbenzo[1,2-*d*:4,5-*d*′]bis([1,3]dithiol-4-yl)-methyl radical. The obtained energy barrier is 13.3 kcal mol^{-1} at the B3LYP/6-31G* level.

Table 3. Computed energy barrier ($\Delta E^{\ddagger}$) to isomerization for **1d** and **2d** (energies are in kcal mol^{-1} relative to reactants).

Mechanism	**1d**	**2d**
Two-ring flip	28.9	30.3
Three-ring flip	73.6	82.4

The computed energy barrier to isomerization is lower for radical **1d** than for its alcohol analogue **2d** (the computed energy barriers in solution are 27.6 and 30.2 kcal mol^{-1}, respectively; Table 4).[28] Calculations of the activation free energy show, however, that the isomerization of radical **1d** is entropically disfavoured: inclusion of zero-point energy, thermal and entropic contributions increases the barrier by 2.7 kcal mol^{-1}. For alcohol **2d** these contributions are much lower (0.3 kcal mol^{-1}). The result of this is that, although the energy barrier is slightly lower for radical **1d**, the barrier to isomerization is similar, in terms of free energy, for both nonsubstituted derivatives (**1d** and **2d**).

In order to investigate the influence of *para* substitution on the aromatic moieties, we computed the energy barrier to isomerization for **1b** and **2b**. Substitution was found to have no significant effect on the rate of interconversion of alcohol derivatives. This is in good agreement with our experimental results, which showed that the free activation energies for **2d** and **2c** are 24.4 and 24.6 kcal mol^{-1}, respectively. The energy barrier to helicity reversal for paramagnetic derivatives is, on the contrary, sensitive to *para* substitution: ester-substituted radical derivative **1b** is computed to be less reactive (energy barrier increased by 1.8 kcal mol^{-1}) than its non-*para*-substituted analogue **1d**. Whereas no difference in reactivity between radical and alcohol is predicted for nonsubstituted derivatives, the rate of isomerization for ester-substituted radical **1b** should thus be lower than for its alcohol analogue **2b**. Indeed, experiments showed that the rate of isomerization is one order of magnitude lower for the ester-substituted paramagnetic derivative **1c**, as compared to that of alcohol derivative **2c**.

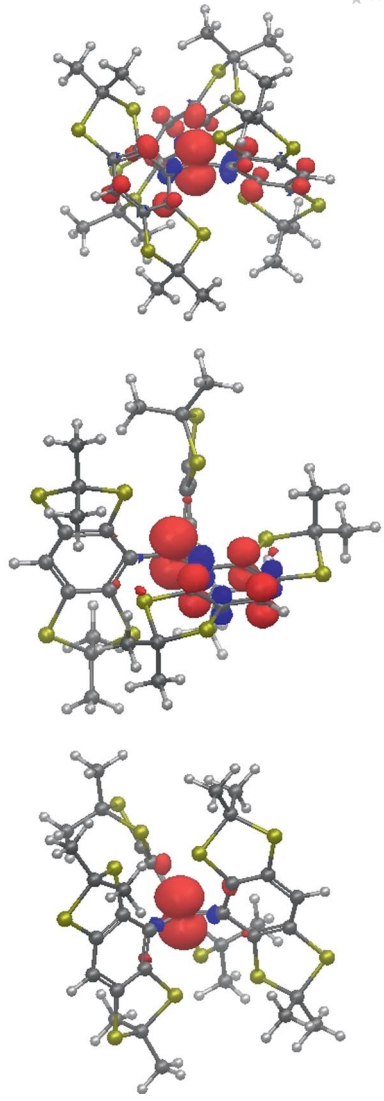

Figure 11. Spin-density surface of ground state (top) and TS for two-ring (center) and three-ring (bottom) flip mechanisms for **1d**.

Table 4. Computed energy barrier ($\Delta E^{\ddagger}$) and activation free energy ($\Delta G^{\ddagger}$) to isomerization (energies are in kcal mol^{-1} relative to reactants).

Compd.	R X	$\Delta E^{\ddagger}$	$\Delta E^{\ddagger}_{(AcOEt)}$	$\Delta G^{\ddagger}_{(EtOAc)}$
1d	R = H X = single electron	28.9	27.6	30.3
1b	R = CO_2Me X = single electron	30.1	29.4	
2d	R = H X = OH	30.3	30.2	30.5
2b	R = CO_2Me X = OH	30.6	30.5	

Conclusions

Tris(tetrathioaryl)methanols, radicals and tris(tetrathioaryl)methanes adopt a propeller-like conformation. Slow interconversion of right-handed (*P*) and left-handed (*M*) propellers is responsible for the chirality of these mole-

cules at room temperature. Analytical and semipreparative CSP-HPLC allows resolution of enantiomers for methanol, radical and methane derivatives. The enantiomerization free activation energies determined by kinetics of racemization using CSP-HPLC vary from 24.4 kcal mol^{-1} for alcohol **2d** to 26.4 kcal mol^{-1} for radical **1c**. Computational chemistry results are in good agreement with the experimental results and show an influence of the *para* substitution for the paramagnetic derivatives; no significant effect was found for the methanol derivatives. Computational and NOESY/EXSY spectroscopy studies are consistent with a two-ring flip mechanism for the isomerization process of tris(tetrathioaryl)methanols, radicals and tris(tetrathioaryl)methanes.

Experimental Section

General: All commercially available reagents were used as received without further purification. NMR spectra were recorded with a Bruker Avance DPX (^{1}H: 500 MHz; ^{13}C: 125 MHz). Chemical shifts (δ) are reported in parts per million (ppm), referenced to NMR solvents, [D]chloroform [δ(^{1}H) = 7.27 ppm, δ(^{13}C) = 77.2 ppm], [D$_6$]dimethyl sulfoxide [δ(^{1}H) = 2.50 ppm, δ(^{13}C) = 39.52 ppm]. The following abbreviations are used: s = singlet, d = doublet, t = triplet, m = multiplet. Coupling constants (J) are reported in Hertz (Hz). HRMS analyses were performed at the University College London. Analytical HPLC was carried out with a Waters Alliance 2690 separations module equipped with a Waters 2998 photodiode array (PDA) detector. Semipreparative reverse-phase HPLC of **3c** was carried out with a Waters 600 Pump equipped with a Waters 486 UV detector, a Waters fraction collector III and a Hitachi L-7200 HPLC autosampler. Semipreparative CSP HPLC was carried out with a Waters 600 Pump equipped with a Waters 996 PDA, a Waters 717 autosampler and a Waters fraction collector III.

Computational Methods: Computations have been performed by using the Jaguar 7.5 pseudospectral program package.[29] All species have been fully optimized, and the Cartesian coordinates are supplied in the Supporting Information. Geometry optimization was performed using the well-established UB3LYP hybrid density functional[30,31] as implemented in Jaguar with the standard split valence polarized 6-31G* basis.[32] This methodology has already been shown to describe properly these systems.[26] Vibrational frequencies were computed for all stationary points for nonsubstituted derivatives (R = H) **1d** and **2d** at the UB3LYP/6-31G* level of theory and are used to include zero-point energy, thermal and entropic corrections to compute ideal-gas free energies. The correct nature of stationary points was confirmed by checking the curvature and its eigenvectors. Ground-state structures were found to be minima with zero imaginary frequency, whereas transition-state structures were found to be first-order saddle points with a single imaginary frequency. Solvation effects were estimated by performing additional single-point energy calculations (UB3LYP/6-31G*) using the Poisson–Boltzmann polarizable continuum method and the parameters appropriate for ethyl acetate (probe radius = 2.69; dielectric constant = 6.02), the solvent used for racemization kinetics. For the large reaction systems there are usually several local minima or saddle points corresponding to each intermediate or transition state. This is due to the possibility of multiple conformations. In particular, the nonplanarity of the two five-membered rings on each phenyl groups allows two different conformations for each ring. Test calculations showed that the energy differences between the various accessible conformers[33] and the energy barriers connecting them are much lower than the barriers to enantiomerization. We have made a systematic attempt to locate all possible local saddle points, with the data presented referring to the lowest energy form.

X-ray Structure Determination: Crystals suitable for X-ray analysis were obtained by slow solvent evaporation from THF solutions. A colourless plate-like crystal (0.24 × 0.410 × 0.04 mm) was flash-cooled in a 120 K nitrogen flow prior to the diffraction experiment. A total of 91 images ($\Delta\phi$ = 2°) were collected with a Mar345 image plate using Mo-K_α radiation (Rigaku UltraX 18 rotating anode). The reflections of the images were indexed and integrated using the CrysalisPro package (Agilent Technologies).[34] Data were scaled and corrected for absorption using the integrated scale3 abspack procedure. The structure was solved by direct methods (SHELXS) and refined by full-matrix least-squares on $|F^2|$ (SHELXL).[35] Non-hydrogen atoms were anisotropically refined, and the hydrogen atoms were placed on calculated positions with temperature factors fixed at 1.2 times U_{eq} of the parent atoms and 1.5 times U_{eq} for methyl groups. The structure was twinned around the reciprocal c axis and was integrated as such. The ratio of both twin domains refined to 48.5%. Crystal Data for **2d**: $C_{37}H_{40}OS_{12}$·2(C_4H_8O), M_r = 1029.62 g mol^{-1}, monoclinic, space group $P2_1/c$, a = 14.0782(11), b = 12.6254(8), c = 27.718(4) Å, β = 98.575(11)°, V = 4871.6(8) Å^3, Z = 4, ρ = 1.404 g cm^{-3}, μ(Mo-K_α) = 0.578 mm^{-1}, T = 120 K, reflections: 11216 collected, 11216 unique, R_{int} = unmerged, R_1 [$|F| > 2\sigma(F)$] = 0.0736, wR_2 [$|F| > 2\sigma(F)$] = 0.1683. CCDC-883661 contains the supplementary crystallographic data for this paper. These data can be obtained free of charge from The Cambridge Crystallographic Data Centre via www.ccdc.cam.ac.uk/data_request/cif.

Tris(8-ethoxycarbonyl-2,2,6,6-tetramethylbenzo[1,2-*d*;4,5-*d*′]bis[1,3]-dithiol-4-yl)methane: To the tris(tetrathioaryl)methanol **2c** (25 mg, 0.023 mmol) was added TFA (5 mL) and metallic zinc foil (120 mg), and the solution was stirred for 48 h. The TFA was then removed under reduced pressure, and the crude product was purified by semipreparative HPLC to give 12.5 mg (50%) of the title compound as an orange solid. The purification conditions were as follows: Column XBridge Prep C18 (10 × 100 mm 5 μm) equipped with a guard column XBridge Prep C18 (10 × 20 mm 5 μm), helium sparge 30 mL/min, UV detection at 267 nm, flow rate: 5 mL/min, eluent: MeCN 86%/H_2O 14%. ^{1}H NMR (500 MHz, $CDCl_3$): δ = 1.47 (t, J = 7.1 Hz, 9 H, OCH_2CH_3), 1.67 (s, 9 H, CH_3), 1.73 (s, 9 H, CH_3), 1.77 (s, 9 H, CH_3), 1.79 (s, 9 H, CH_3), 4.35–4.50 (m, 6 H, OCH_2CH_3), 5.39 (s, 1 H, C*H*) ppm. ^{13}C NMR (125 MHz, $CDCl_3$): δ = 14.5 (OCH_2CH_3), 29.0 (CH_3), 29.3 (CH_3), 33.0 (CH_3), 34.2 (CH_3), 62.2 (*C*H), 62.3 (S*C*S), 62.5 (OCH_2CH_3), 62.9 (S*C*S), 120.4 (*C*Ar), 130.0 (*C*Ar), 139.3 (*C*Ar), 140.1 (*C*Ar), 140.6 (*C*Ar), 141.8 (*C*Ar), 166.5 ($CO_2CH_2CH_3$) ppm. HRMS (TOF MS ES+): calcd. for $C_{46}H_{53}O_6S_{12}$ [M + H]$^+$ 1085.0491; found 1085.0607. RP HPLC: t_R = 6.14 min [254 nm, 1 mL/min, MeCN 100%, Symmetry C18 (4.6 × 250 mm), 25 °C].

Exchange Spectroscopy: The 2D ^{1}H-^{1}H NOESY/EXSY was recorded at 145 °C using the Bruker noesygpph pulse sequence, mixing time d8 = 0.6 s, spectral width SW = 0.5 ppm, centre of spectrum O1P = 1.71 ppm, TD = 1024 points in the direct-detect ^{1}H dimension, TD = 256 increments in the indirect ^{1}H dimension, number of scans ns = 32, number of dummy scans ds = 16. A sine bell window function shifted by 90° was used to process both dimensions of the spectrum. Zero filling was used to obtain a final resolution of 0.12 Hz/point in the direct ^{1}H dimension and 0.24 Hz/point in the indirect ^{1}H dimension.

Resolution of Enantiomers: The two enantiomers of **2c** were separated by using a procedure previously reported.[26] Enantiomers of **3c** were separated by using a semipreparative CHIRALPAK IB column 10 × 250 mm 5 μm equipped with a guard column CHIRALPAK IB 10 × 20 mm 5 μm. The conditions of resolution were as follows: flow rate: 4.7 mL/min; eluent: isohexane 88%/EtOAc 10%/EtOH 2%. UV detection: 268 nm; column temperature: ambient. Enantiomers of **2d** were separated with an analytical CHIRALPAK IA column 4.6 × 250 mm 5 μm equipped with a guard column CHIRALPAK IA 4.6 × 20 mm 5 μm. The conditions of resolution were as follows: flow rate: 1 mL/min; eluent: isohexane 88%/EtOAc 10%/EtOH 2%. UV detection: 275 nm; column temperature: ambient. Enantiomers of **2c**, **2d**, **3c** were collected using a fraction collector in a flask cooled to –78 °C.

HPLC Kinetics: The racemizations of **2c**, **2d** and **3c** were monitored by CSP HPLC according to this general procedure: one enantiomer was dissolved with EtOAc at 25 °C in an HPLC vial (1.5 mL). The vial was then placed in the HPLC oven where the temperature was controlled to 25 °C. This time was considered to be $t = 0$. Chromatograms were recorded periodically over the time and the enantiomeric excess was calculated by integration of the two enantiomers at 274 nm for **2c**, 274 nm for **2d** and 267 nm for **3c**. Kinetic measurements were stopped when % *ee* = 0. The conditions of resolution were as follows: For **2c**: Column: CHIRALPAK IB (4.6 × 250 mm 5 μm) equipped with a guard column CHIRALPAK IB (4.6 × 20 mm 5 μm), flow rate: 1 mL/min; eluent: isohexane 93%/EtOAc 4%/MeOH 3%. For **2d**: Column: CHIRALPAK IA (4.6 × 250 mm 5 μm) equipped with a guard column CHIRALPAK IA (4.6 × 20 mm 5 μm), flow rate: 0.5 mL/min; eluent: isohexane 90%/EtOAc 7%/EtOH 3%. For **3c**: Column: CHIRALPAK IB (4.6 × 250 mm 5 μm) equipped with a guard column CHIRALPAK IB (4.6 × 20 mm 5 μm), flow rate: 1 mL/min; eluent: isohexane 88%/EtOAc 10%/EtOH 2%.

Supporting Information (see footnote on the first page of this article): ^{1}H NMR, ^{13}C NMR, HR mass spectra and HPLC chromatogram of **3c**; optimized Cartesian coordinates and corresponding energies for all species discussed in the text.

Acknowledgments

This work has been supported by the Université catholique de Louvain (UCL) and the Fonds de la Recherche Scientifique (F. R. S. – FNRS). J. M.-B. and R. R. are Chercheurs qualifiés F. R. S. – FNRS.

[1] D. J. Lurie, H. Li, S. Petryakov, J. L. Zweier, *Magn. Reson. Med.* **2002**, *47*, 181–186.
[2] J. H. Ardenkjær-Larsen, I. Laursen, I. Leunbach, G. Ehnholm, L. G. Wistrand, J. S. Petersson, K. Golman, *J. Magn. Reson.* **1998**, *133*, 1–12.
[3] S. Xia, F. A. Villamena, C. M. Hadad, P. Kuppusamy, Y. Li, H. Zhu, J. L. Zweier, *J. Org. Chem.* **2006**, *71*, 7268–7279.
[4] Y. Deng, S. Petryakov, G. He, E. Kesselring, P. Kuppusamy, J. L. Zweier, *J. Magn. Reson.* **2007**, *185*, 283–290.
[5] N. Charlier, B. Driesschaert, N. Wauthoz, N. Beghein, V. Préat, K. Amighi, J. Marchand-Brynaert, B. Gallez, *J. Magn. Reson.* **2009**, *197*, 176–180.
[6] I. Dhimitruka, A. A. Bobko, C. M. Hadad, J. L. Zweier, V. V. Khramtsov, *J. Am. Chem. Soc.* **2008**, *130*, 10780–10787.
[7] B. Driesschaert, V. Marchand, P. Leveque, B. Gallez, J. Marchand-Brynaert, *Chem. Commun.* **2012**, *48*, 4049–4051.
[8] Y. Liu, Y. Song, A. Rockenbauer, J. Sun, C. Hemann, F. A. Villamena, J. L. Zweier, *J. Org. Chem.* **2011**, *76*, 3853–3860.
[9] C. Rizzi, A. Samouilov, V. K. Kutala, N. L. Parinandi, J. L. Zweier, P. Kuppusamy, *Free Radical Biol. Med.* **2003**, *35*, 1608–1618.
[10] Y. Liu, F. A. Villamena, Y. Song, J. Sun, A. Rockenbauer, J. L. Zweier, *J. Org. Chem.* **2010**, *75*, 7796–7802.
[11] M. H. Lerche, S. Meier, P. R. Jensen, H. Baumann, B. O. Petersen, M. Karlsson, J. Ø. Duus, J. H. Ardenkjær-Larsen, *J. Magn. Reson.* **2010**, *203*, 52–56.
[12] G. N. Lewis, D. Lipkin, T. T. Magel, *J. Am. Chem. Soc.* **1944**, *66*, 1579–1583.
[13] P. Andersen, B. Klewe, *Acta Chem. Scand.* **1967**, *21*, 2599–2607.
[14] K. Schreiner, A. Berndt, F. Baer, *Mol. Phys.* **1973**, *26*, 929–939.
[15] Y. Liu, F. A. Villamena, J. Sun, Y. Xu, I. Dhimitruka, J. L. Zweier, *J. Org. Chem.* **2008**, *73*, 1490–1497.
[16] D. Gust, K. Mislow, *J. Am. Chem. Soc.* **1973**, *95*, 1535–1547.
[17] Y. Okamoto, E. Yashima, K. Hatada, K. Mislow, *J. Org. Chem.* **1984**, *49*, 557–558.
[18] V. Bobosik, C. Lopez, R. M. Claramunt, C. Roussel, J. L. Stein, D. Thiery, J. Elguero, *Heterocycles* **1993**, *35*, 1067–1074.
[19] B. Driesschaert, N. Charlier, B. Gallez, J. Marchand-Brynaert, *Bioorg. Med. Chem. Lett.* **2008**, *18*, 4291–4293.
[20] S. Macholl, H. Johannesson, J. H. Ardenkjaer-Larsen, *Phys. Chem. Chem. Phys.* **2010**, *12*, 5804–5817.
[21] V. M. Tormyshev, A. M. Genaev, G. E. Sal′nikov, O. Y. Rogozhnikova, T. I. Troitskaya, D. V. Trukhin, V. I. Mamatyuk, D. S. Fadeev, H. J. Halpern, *Eur. J. Org. Chem.* **2012**, 623–629.
[22] C. Decroos, Y. Li, G. Bertho, Y. Frapart, D. Mansuy, J.-L. Boucher, *Chem. Res. Toxicol.* **2009**, *22*, 1342–1350.
[23] T. J. Reddy, T. Iwama, H. J. Halpern, V. H. Rawal, *J. Org. Chem.* **2002**, *67*, 4635–4639.
[24] I. Dhimitruka, M. Velayutham, A. A. Bobko, V. V. Khramtsov, F. A. Villamena, C. M. Hadad, J. L. Zweier, *Bioorg. Med. Chem. Lett.* **2007**, *17*, 6801–6805.
[25] C. Decroos, T. Prange, D. Mansuy, J.-L. Boucher, Y. Li, *Chem. Commun.* **2011**, *47*, 4805–4807.
[26] B. Driesschaert, R. Robiette, F. Lucaccioni, B. Gallez, J. Marchand-Brynaert, *Chem. Commun.* **2011**, *47*, 4793–4795.
[27] S. Ito, N. Morita, T. Asao, *Bull. Chem. Soc. Jpn.* **1995**, *68*, 1409–1436.
[28] Computed energy barriers reveal a systematic overestimation of barriers height by this method. Such systematic errors in the estimation of energy barriers are well known (see: D. A. Goldfeld, A. D. Bochevarov, R. A. Friesner, *J. Chem. Phys.* **2008**, *129*, 214105–13). Because of the similarity between all the studied systems, these errors are expected to cancel out, and relative rates should be reliable.
[29] *Jaguar*, version 7.5, Schrödinger, LLC, New York, **2008**.
[30] A. D. Becke, *J. Chem. Phys.* **1993**, *98*, 5648–5652.
[31] M. M. Francl, W. J. Pietro, W. J. Hehre, J. S. Binkley, M. S. Gordon, D. J. DeFrees, J. A. Pople, *J. Chem. Phys.* **1982**, *77*, 3654–3665.
[32] W. J. Hehre, R. Ditchfield, J. A. Pople, *J. Chem. Phys.* **1972**, *56*, 2257–2261.
[33] In most cases, the more stable conformer is the one in which the five-membered rings on each phenyl group are twisted in opposite directions so that the whole substituted phenyl group is in a chair-like conformation.
[34] Xcalibur CCD system, CrysAlisPro Software system, Version 1.171.35.19, Agilent Technologies XRD, Agilent Technologies, **2010**.
[35] G. M. Sheldrick, *Acta Crystallogr., Sect. A* **2008**, *64*, 112–122.

Received: June 15, 2012
Published Online: August 9, 2012

